Wavelets and Multiresolution Transforms with Applications

- Some theory and description of the algorithms
- Lots of examples of applications
- Astronomy, Earth observation, forensics, financial time series modeling, medical imaging, …

1

Some Examples of Wavelet Transforms in Operation

1) Visualization – comet core

2) Separating objects on different scales – galaxy vis-à-vis stars

3) Intelligent background removal – ecstasy tablets

4) SeaWiFS image of Gulf of Aden: eddies, current in colour data → biomass

2

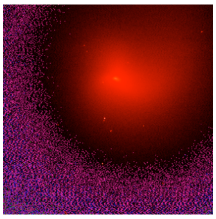

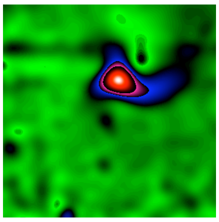

Left: Periodic comet P/Swift-Tuttle observed with the 1.2m telescope at Calar Alto Observatory in Spain in October and November 1992. (Data courtesy of Dr K Birkle, Max-Planck-Institut für Astronomie, Heidelberg).
Irregularity of nucleus is indicative of the presence of jets in in the coma.
Right: Scale 5 of a B3 spline à trous wavelet transform.

3

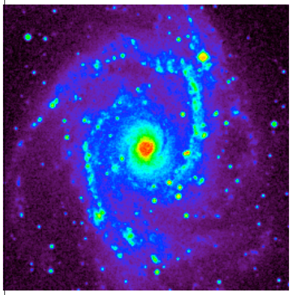

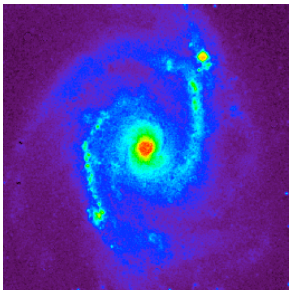

4

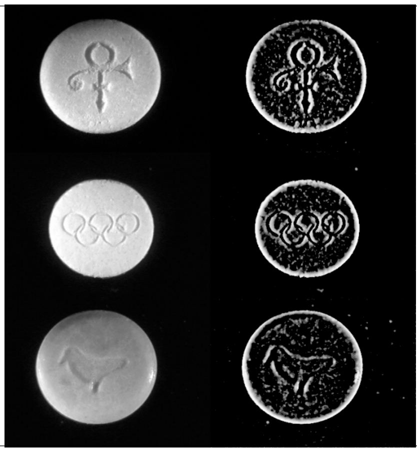

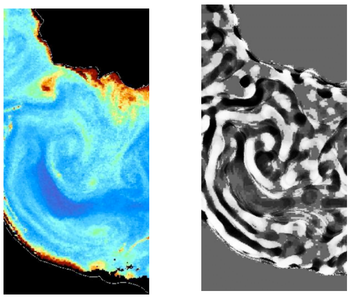

Motivation for Multiscale Methods:
Take the Case of:
Astronomical Data Analysis

- Tendency is away from specialized treatment of a particular object or even class of object, and is instead towards:
- Surveys, and (semi) automated analysis of ensembles of object and families of object, based on a compact "collaboratory" or virtual community, characterized as the virtual observatory.

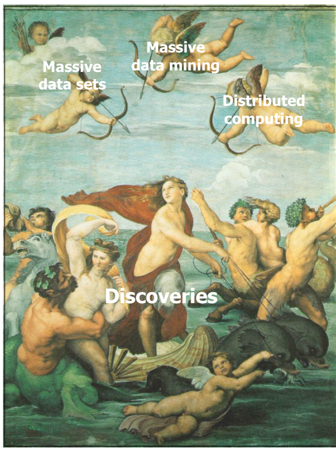

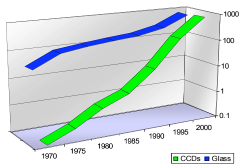

Hardware breakthrough:
wide field imaging with CCD mosaics enables digital surveys

The sky covers 40,000 sq. deg.
with 0.6 arcsec sampling: 2 x 10^{12} pel
8 TB for a band (10/100 TB/survey)
Ca. **10 PB** keeping temporal resolution

➢From Traditional to Survey Science

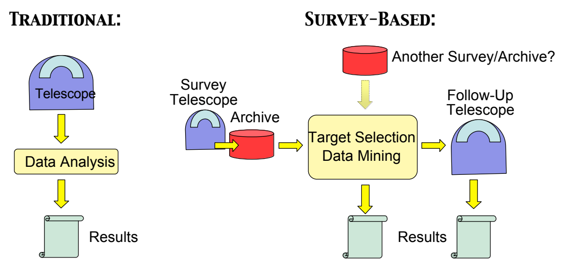

Highly successful and increasingly prominent, but inherently limited by the information content of individual surveys …

__What comes next, beyond survey science is distributed (V.O.) science__

9

Courtesy of G. Djorgovski

Panchromatic view of the Universe:

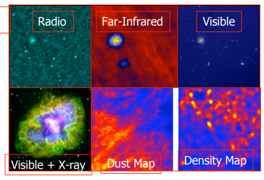

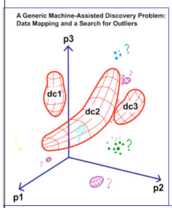

Search for the unknown

Offers:
Different physics
Global understanding
Comparison with theory
New discoveries

New domains of the parameter space: cf. time

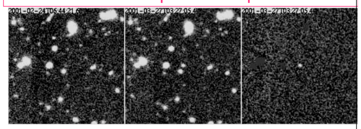

Faint, fast transients

10

---

1. Introduction
2. The Continuous Wavelet Transform
3. The Discrete Wavelet Transform
4. Noise Modeling in Wavelet Space
5. Examples and Demonstrations
6. Applications
   (a) Filtering
   (b) Deconvolution
   (c) Compression
   (d) Detection
   (e) Image Registration

The Continuous Wavelet Transform

$$W(a,b) = K \int_{-\infty}^{+\infty} \psi^*(\frac{x-b}{a}) f(x) dx$$

where:

- $W(a,b)$ is the wavelet coefficient of the function $f(x)$
- $\psi(x)$ is the analyzing wavelet
- a (> 0) is the scale parameter
- b is the position parameter

In Fourier space, we have: $\hat{W}(a,\nu) = \sqrt{a}\hat{f}(\nu)\hat{\psi}^*(a\nu)$
When the scale a varies, the filter $\hat{\psi}^*(a\nu)$ is only reduced or dilated while keeping the same pattern.

Properties

- CWT is a linear transformation:
  - if $f(x) = f_1(x) + f_2(x)$ then $W_f(a,b) = W_{f_1}(a,b) + W_{f_2}(a,b)$
  - if $f(x) = kf_1(x))$ then $W_f(a,b) = kW_{f_1}(a,b)$
- CWT is covariant under translation:

  if $f_0(x) = f(x - x_0)$ then $W_{f_0}(a,b) = W_f(a, b - x_0)$
- CWT is covariant under dilation:

  if $f_s(x) = f(sx)$ then $W_{f_s}(a,b) = \frac{1}{s^{\frac{1}{2}}} W_f(sa, sb)$

Whatever the scale and the position, the signal analysis is done using the same function.

The Inverse Transform

The inverse transform is:

$$f(x) = \frac{1}{C_\psi} \int_{-\infty}^{+\infty} \int_0^{+\infty} \frac{1}{\sqrt{a}} W(a,b) \psi(\frac{x-b}{a}) \frac{da db}{a^2}$$

where

$$C_\psi = \int_{-\infty}^{+\infty} \mid \hat{\psi}(t) \mid^2 \frac{dt}{t} < +\infty$$

Reconstruction is only possible if C_ψ is defined (admissibility condition). This condition implies $\hat{\psi}(0) = 0$, i.e. the mean of the wavelet function is 0.

Mexican hat

The Mexican hat function is in one dimension:

$$g(x) = (1 - x^2) e^{-\frac{1}{2}x^2}$$

This is the second derivative of a Gaussian.

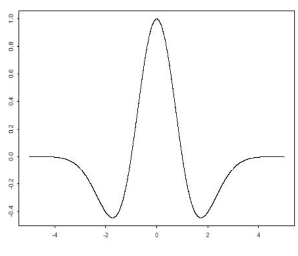

Multiresolution Analysis

Multiresolution analysis (Mallat, 1989) results from the embedded subsets generated by the interpolations at different scales.

A function $f(x)$ is projected at each step j onto the subset V_j $(\ldots \subset V_{2^{j+1}} \subset V_{2^j} \subset V_{2^{j-1}} \subset V_{2^0} \ldots)$. This projection is defined by the scalar product $c_j(k)$ of $f(x)$ with the scaling function $\phi(x)$ which is dilated and translated:

$$c_j(x) \quad = \quad < f(x), \phi_j(x - 2^j k) >$$

$$\phi_j(x) = 2^j \phi(2^j x)$$

where $\phi(x)$ is the scaling function. ϕ is a low-pass filter.

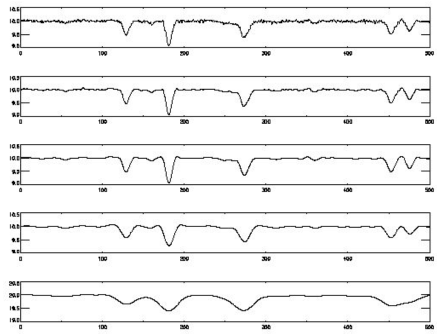

Wavelets and Multiresolution Analysis

The difference between c_{j-1} and c_j is contained in the detail signal belonging to the space O_j orthogonal to V_j.

$$O_j \oplus V_j = V_{j-1}$$

The set $\sqrt{2^{-j}}\psi_j(x - 2^{-j}k)_{k \in \mathcal{Z}}$ forms a basis of O_j.

$$\psi_j(x) = 2^j \psi(2^j x)$$

where $\psi(x)$ is the wavelet function.

The wavelet coefficients are obtained by:

$$w_j(x) \quad = \quad < f(x), \psi_j(x - 2^j k) >$$

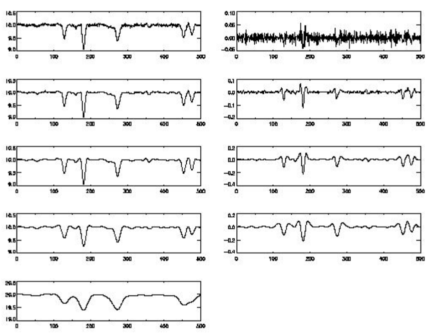

A few remarks…

- On 2D images, the algorithm may be carried out in a genuinely 2D way, but this may have a computational overhead. Separability (in x and y) is often used instead. The same principle applies for 3D image volumes.
- Because the signal is increasingly smooth, we can keep one sample out of two. This is called decimation. It is crucial in compression applications. Exact reconstruction is guaranteed. But for signal detection type applications, it can lead to aliasing if we interpret/analyze the data in the wavelet transform space.
- For general wavelet functions, we need to reverse the effects of transforming, when carrying out the inverse transform. The Haar WT is orthogonal and leads to a particularly simple algorithm. A more general algorithm is the biorthogonal WT.

20

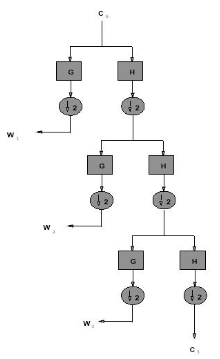

Keep one sample out of two

21

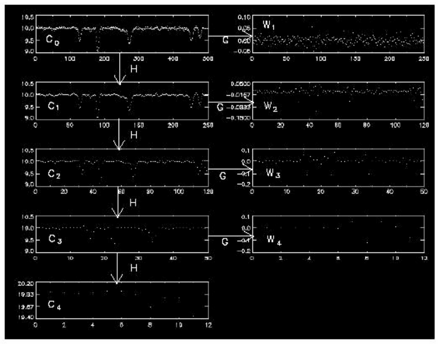

Pyramidal Algorithm

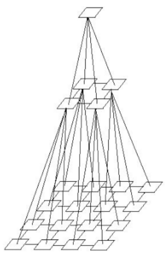

Several algorithms exist:

- The Laplacian Pyramid
- Pyramid with one wavelet
- Pyramidal wavelet transform using the FFT

23

NGC 2997 pyramidal coefficients

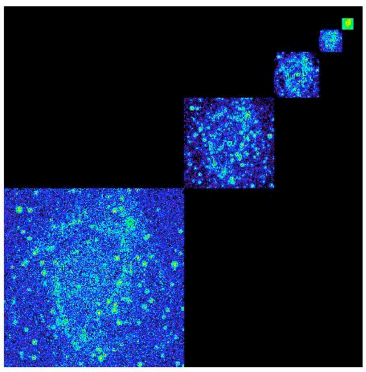

24

Next…

1. Biorthogonal wavelets
2. Orthogonal wavelets
3. Feauveau transform
4. Wavelet packets
5. Lifting scheme
6. Integer transform
7. A trous transform
8. Multiresolution median transform (non-wavelet)
9. Noise and noise modeling

Reconstruction with bi-orthogonal wavelets

Two other filters $\tilde{h}$ and $\tilde{g}$ are used, defined to be conjugate to h and g. The reconstruction of the signal is performed with:

$$c_j(k) = 2\sum_l [c_{j+1}(l)\tilde{h}(k-2l) + w_{j+1}(l)\tilde{g}(k-2l)]$$

In order to get an exact reconstruction, two conditions are required for the conjugate filters:

- *Dealiasing condition:* $\hat{h}(\nu + \frac{1}{2})\hat{\tilde{h}}(\nu) + \hat{g}(\nu + \frac{1}{2})\hat{\tilde{g}}(\nu) = 0$
- *Exact restoration:* $\hat{h}(\nu)\hat{\tilde{h}}(\nu) + \hat{g}(\nu)\hat{\tilde{g}}(\nu) = 1$

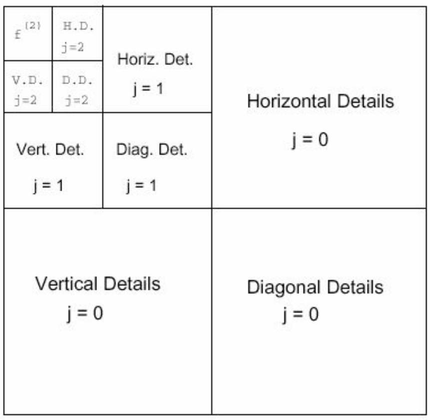

In two dimensions, we separate the variables x, y:

- vertical wavelet: $\psi^1(x,y) = \phi(x)\psi(y)$
- horizontal wavelet: $\psi^2(x,y) = \psi(x)\phi(y)$
- diagonal wavelet: $\psi^3(x,y) = \psi(x)\psi(y)$

The detail signal is contained in three sub-images:

$$\begin{aligned}
w_j^1(k_x,k_y) &= \sum_{l_x=-\infty}^{+\infty}\sum_{l_y=-\infty}^{+\infty} g(l_x - 2k_x)h(l_y - 2k_y)c_{j+1}(l_x,l_y) \\
w_j^2(k_x,k_y) &= \sum_{l_x=-\infty}^{+\infty}\sum_{l_y=-\infty}^{+\infty} h(l_x - 2k_x)g(l_y - 2k_y)c_{j+1}(l_x,l_y) \\
w_j^3(k_x,k_y) &= \sum_{l_x=-\infty}^{+\infty}\sum_{l_y=-\infty}^{+\infty} g(l_x - 2k_x)g(l_y - 2k_y)c_{j+1}(l_x,l_y)
\end{aligned}$$

29

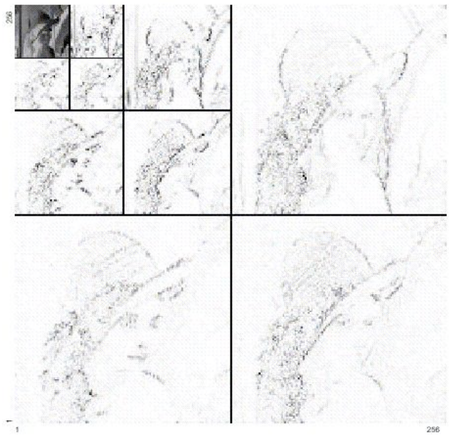

30

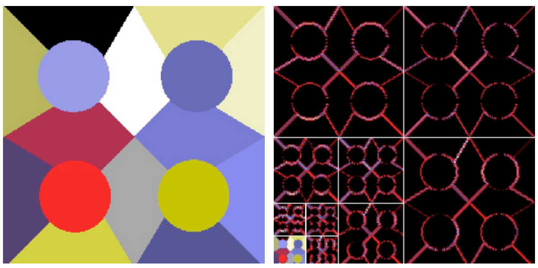

31

Orthogonal wavelets

Orthogonal wavelets correspond to the restricted case where:

$$\begin{aligned}\hat{g}(\nu) &= e^{-2\pi i\nu}\hat{h}^*(\nu+\frac{1}{2})\\ \hat{\tilde{h}}(\nu) &= \hat{h}^*(\nu)\\ \hat{\tilde{g}}(\nu) &= \hat{g}^*(\nu)\end{aligned}$$

and $\mid \hat{h}(\nu) \mid^2 + \mid \hat{h}(\nu+\frac{1}{2}) \mid^2 = 1$

Then we have $g(n) = (-1)^{1-n}h(1-n)$.

$g(n)$ and $h(n)$ are called Conjugate Mirror Filters.

Example: the Haar Wavelet Transform

$$\psi(x) = 1 \quad \text{if } 0 \leq x < \tfrac{1}{2}$$
$$\psi(x) = -1 \quad \text{if } \tfrac{1}{2} \leq x < 1$$
$$\psi(x) = 0 \quad \text{otherwise}$$

And $\phi(x) = 1$ for $0 \leq x < 1$

Latter is low-pass (averaging) filter

y is band-pass (differencing) filter

Both are translated and dilated for the Haar WT

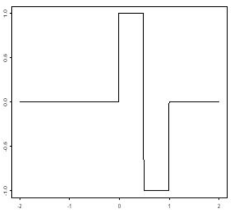

33

Input signal on top.
Haar WT algorithm follows.
Bottom line: Haar WT.

64	48	16	32	56	56	48	24
56	24	56	36	**8**	**-8**	**0**	**12**
40	46	**16**	**10**	**8**	**-8**	**0**	**12**
43	**-3**	**16**	**10**	**8**	**-8**	**0**	**12**

56 = average of 65 and 48; and +8 or -8 is needed to recreate inputs.
24 = average of 16 and 32; and -8 or -(-8) is needed to recreate inputs.
At scale 2, detail coefficients 8, -8, 0, 12 are just repeated.
At scale 3, detail coefficients 16, 10, 8, -8, 0, 12 are just repeated.

34

Non-Dyadic Resolution Factor

Feauveau introduced *quincunx* analysis. This analysis is not dyadic and allows an image decomposition with a resolution factor equal to $\sqrt{2}$.

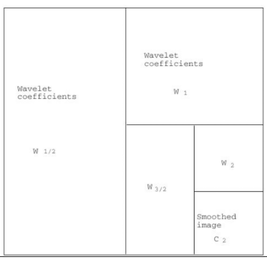

35

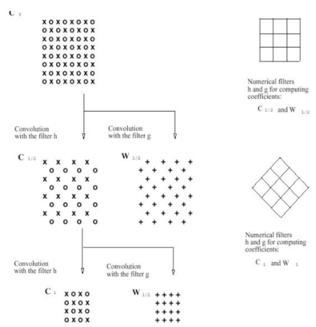

At each step, the image is undersampled by two in one direction (x and y, alternatively). This undersampling is made by keeping one pixel out of two, alternatively even and odd.

36

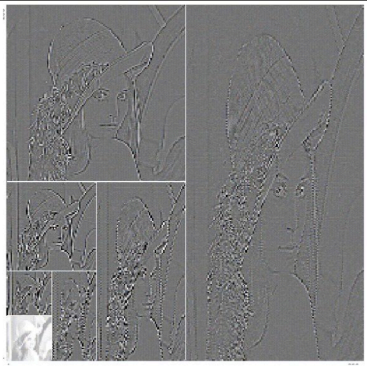

Figure 1: Wavelet transform of Lena by Feauveau's algorithm.

37

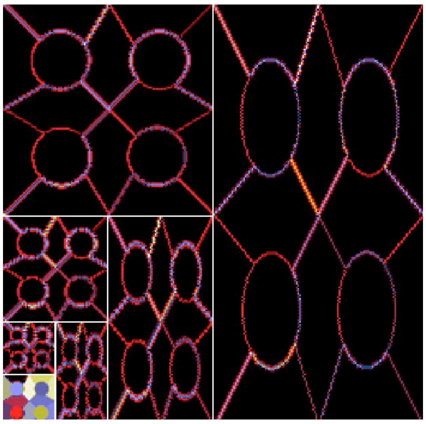

38

Wavelet Packet

Wavelet packets were introduced by Coifman, Meyer and Wickerhauser (1992). Instead of dividing only the approximation space, as in the standard orthogonal wavelet transform, detail spaces are also divided.

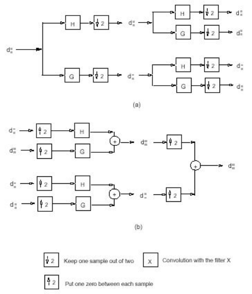

Wavelet packet Scheme: (a) forward direction, (b) reconstruction.

39

Sweldens' lifting scheme - a general wavelet transform algorithm

"... second generation wavelets, i.e. wavelets adapted to situations that do not allow translation and dilation like non-Euclidean spaces. ... A construction using lifting ... is entirely spatial and therefore ideally suited for building second generation wavelets when Fourier techniques are no longer available."

("Factoring wavelet transforms into lifting steps", I Daubechies and W Sweldens, http://cm.bell-labs.com/who/wim/papers/factor/factor.pdf
J. Fourier Anal. Appl., Vol. 4, Nr. 3, pp. 247-269, 1998)

40

Lifting - 2

- Split a signal into its polyphase components: even indexed samples, and odd indexed samples. Typically they are correlated.
- Hence given one, e.g. odd, build a good predictor, P, for the other.
- odd set - P(even set) = detail
- $d = x_o - P(x_e)$
- Given the even and d, we can recover the odd:
- $x_o = P(x_e) | d$
- If P is a good predictor, then d is sparse, i.e. we expect entropy of d to be smaller than entropy of x_o.

41

Lifting - 3

Example:

- d_k = x_{2k+1} - (x_{2k} + x_{2k+2})/2
- Here we are taking a predictor of an odd from its even neighbours.
- If signal is locally linear, then d_k is zero. This is the lifting step.
- So far, we have a transform from (x_e, x_o) to (x_e, d).
- Difficulty: x_e was obtained from subsampling, so serious aliasing occurs. So we apply a second lifting step.

42

Lifting - 4

- The evens are replaced with smoothed values using an update operator, U, applied to the details:
- s = x_e | U(d)
- Then we can invert:
- x_e = s - U(d)
- and that in turn allows us to recover x_o.
- In our example we have:
- s_k = x_{2k} + (d_{k-1} + d_k)/4

43

Lifting - 5

- With more general prediction functions, then for irregular sampling,the sphere, or more complex manifolds, we can use this.
- Greater efficiency of calculation results for long filters. Integer transforms are possible.

44

Lifting Scheme Transformation in Three Steps:

1. Split the signal into even- and odd-numbered samples: $c_{j+1,l} = c_{j,2l}$ and $w_{j+1,l} = c_{j,2l+1}$.
2. Set $w_{j+1,l} = w_{j+1,l} - \mathcal{P}(c_{j+1,l})$
3. Set $c_{j+1,l} = c_{j+1,l} + \mathcal{U}(w_{j+1,l})$

where $\mathcal{U}$ is the update operator.

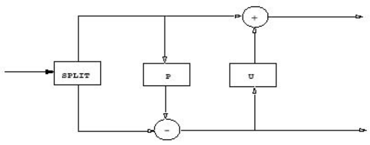

The Lifting Scheme - forward direction.

Reconstruction

Reconstruction is obtained by:

$$\begin{aligned} c_{j,2l} &= c_{j+1,l} - \mathcal{U}(w_{j+1,l}) \\ c_{j,2l+1} &= w_{j+1,l} + \mathcal{P}(c_{j+1,l}) \end{aligned}$$

Haar wavelet via lifting

The Haar transform can be performed via the lifting scheme by taking the predict operator equal to the identity, and an update operator which halves the difference. The transform becomes:

$$\begin{aligned} w_{j+1,l} &= w_{j+1,l} - c_{j+1,l} \\ c_{j+1,l} &= c_{j+1,l} + \frac{w_{j+1,l}}{2} \end{aligned}$$

All computation can be done in place. Every wavelet transform can be written via lifting.

Integer Wavelet Transform

When the input data are integer values, the wavelet transform no longer consists of integers. For lossless coding, however, we need a wavelet transform which produces integer values. We can built an integer version of every wavelet transform. For instance, the integer Haar transform can be calculated by:

$$\begin{aligned} w_{j+1,l} &= c_{j,2l+1} - c_{j,2l} \\ c_{j+1,l} &= c_{j,2l} + \lfloor \frac{w_{j+1,l}}{2} \rfloor = c_{j+1,l} + \lfloor \frac{w_{j+1,l}}{2} \rfloor \end{aligned}$$

and the reconstruction is

$$\begin{aligned} c_{j,2l} &= c_{j+1,l} - \lfloor \frac{w_{j+1,l}}{2} \rfloor \\ c_{j,2l+1} &= w_{j+1,l} + c_{j,2l} \end{aligned}$$

More generally, the lifting operators for an integer version of the wavelet transform are:

$$\begin{aligned} \mathcal{P}(c_{j+1,l}) &= \lfloor \sum_k p_k c_{j+1,l-k} + \frac{1}{2} \rfloor \\ \mathcal{U}(w_{j+1,l}) &= \lfloor \sum_k u_k w_{j+1,l-k} + \frac{1}{2} \rfloor \end{aligned}$$

The linear integer wavelet transform is

$$\begin{aligned} w_{j+1,l} &= w_{j+1,l} - \lfloor \frac{1}{2}(c_{j+1,l} + c_{j+1,l+1}) + \frac{1}{2} \rfloor \\ c_{j+1,l} &= c_{j+1,l} + \lfloor \frac{1}{4}(w_{j+1,l-1} + w_{j+1,l}) + \frac{1}{2} \rfloor \end{aligned}$$

The à trous Algorithm

This is a "stationary" or redundant transform, i.e. decimation is not carried out. The distance between samples increasing by a factor 2 from scale $(j-1)$ $(j>0)$ to the next, $c_j(k)$, is given by:

$$c_j(k) = \sum_l h(l) c_{j-1}(k + 2^{j-1} l)$$

and the discrete wavelet coefficients by:

$$w_j(k) = \sum_l g(l) c_{j-1}(k + 2^{j-1} l)$$

Generally, the wavelet resulting from the difference between two successive approximations is applied:

$$w_j(k) = c_{j-1}(k) - c_j(k)$$

The associated wavelet is $\psi(x)$.

$$\frac{1}{2}\psi(\frac{x}{2}) = \phi(x) - \frac{1}{2}\phi(\frac{x}{2})$$

The reconstruction algorithm is immediate:

$$c_0(k) = c_{n_p}(k) + \sum_{j=1}^{n_p} w_j(k)$$

49

Passage from c_0 to c_1, and from c_1 to c_2

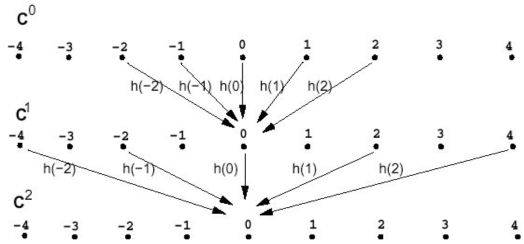

50

The triangle function

Choosing the triangle function as the scaling function ϕ leads to piecewise linear interpolation:

$$\phi(x) = 1 - \mid x \mid \quad \text{if } x \in [-1, 1]$$
$$\phi(x) = 0 \quad \text{if } x \notin [-1, 1]$$

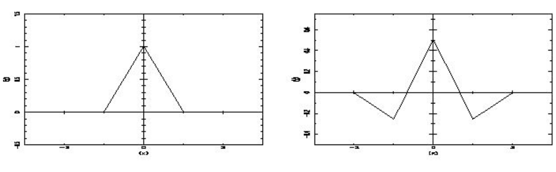

51

We have

$$\frac{1}{2}\phi(\frac{x}{2}) = \frac{1}{4}\phi(x+1) + \frac{1}{2}\phi(x) + \frac{1}{4}\phi(x-1)$$

c_{j+1} is obtained from c_j by:

$$c_{j+1}(k) = \frac{1}{4}c_j(k - 2^j) + \frac{1}{2}c_j(k) + \frac{1}{4}c_j(k + 2^j)$$

The wavelet coefficients at scale j are:

$$w_{j+1}(k) = -\frac{1}{4}c_j(k - 2^j) + \frac{1}{2}c_j(k) - \frac{1}{4}c_j(k + 2^j)$$

52

The cubic spline function

$$B_3(x) = \frac{1}{12}(\mid x-2\mid^3 - 4\mid x-1\mid^3 + 6\mid x\mid^3 - 4\mid x+1\mid^3 + \mid x+2\mid^3)$$

and

$$h(-2) = \frac{1}{16}; h(-1) = \frac{1}{4}; h(0) = \frac{3}{8}; h(1) = \frac{1}{4}; h(2) = \frac{1}{16}$$

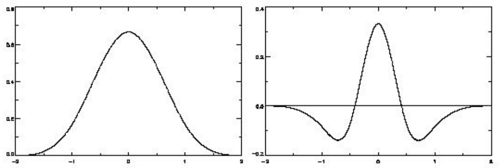

Multiresolution Median Transform

1. Let $c_j = I$ with $j = 1$
2. Determine $c_{j+1} = med(f, 2s+1)$.
3. The multiresolution coefficients w_{j+1} are defined as: $w_{j+1} = c_j - c_{j+1}$.
4. Let $j \longleftarrow j+1$; $s \longleftarrow 2s$. Return to step 2 if $j < S$.

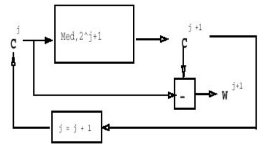

Reconstruction by: $I = c_p + \sum_j w_j$

Pyramidal Median Transform

1. Let $c_j = I$ with $j = 1$.
2. Determine $c^*_{j+1} = med(c_j, 2s+1)$ with $s = 1$.
3. The pyramidal multiresolution coefficients w_{j+1} are defined as:

$$w_{j+1} = c_j - c^*_{j+1}$$

4. Let $c_{j+1} = dec(c^*_{j+1})$ (where the decimation operation, dec, entails 1 pixel replacing each 2×2 subimage).
5. Let $j \longleftarrow j+1$. Return to step 2 so long as $j < S$.

Gaussian Noise

$$p(w_j(x,y)) = \frac{1}{\sqrt{2\pi}\sigma_j} e^{-w_j(x,y)^2/2\sigma_j^2}$$

Rejection of hypothesis $\mathcal{H}_0$ depends (for a positive coefficient value) on:

$$P = Prob(w_j(x,y) > W) = \frac{1}{\sqrt{2\pi}\sigma_j} \int_{w_j(x,y)}^{+\infty} e^{-W^2/2\sigma_j^2} dW$$

and if the coefficient value is negative, it depends on

$$P = Prob(w_j(x,y) < W) = \frac{1}{\sqrt{2\pi}\sigma_j} \int_{-\infty}^{w_j(x,y)} e^{-W^2/2\sigma_j^2} dW$$

Given stationary Gaussian noise, it suffices to compare $w_j(x,y)$ to $k\sigma_j$.

$$\text{if } \mid w_j \mid \geq k\sigma_j \quad \text{then } w_j \text{ is significant}$$
$$\text{if } \mid w_j \mid < k\sigma_j \quad \text{then } w_j \text{ is not significant}$$

How to find σ_j ?

The appropriate value of σ_j in the succession of wavelet planes is assessed from the standard deviation of the noise σ_I in the original image and from study of the noise in wavelet space. This study consists of simulating an image containing Gaussian noise with a standard deviation equal to 1, and taking the wavelet transform of this image. Then we compute the standard deviation σ_j^e at each scale. We get a curve σ_j^e as a function of j, giving the behavior of the noise in wavelet space. (Note that if we had used an orthogonal wavelet transform, this curve would be linear.) Due to the properties of the wavelet transform, we have $\sigma_j = \sigma_I \sigma_j^e$. The standard deviation of the noise at a scale j of the image is equal to the standard deviation of the noise of the image multiplied by the standard deviation of the noise of the scale j of the wavelet transform.

57

Poisson Noise

If the noise in the data I is Poisson, the transform

$$t(I(x,y)) = 2\sqrt{I(x,y) + \frac{3}{8}}$$

acts as if the data arose from a Gaussian white noise model (Anscombe, 1948), with $\sigma = 1$, under the assumption that the mean value of I is large.

Poisson Noise + Gaussian

The generalization of the variance stabilizing is:

$$t(I(x,y)) = \frac{2}{\alpha}\sqrt{\alpha I(x,y) + \frac{3}{8}\alpha^2 + \sigma^2 - \alpha g}$$

where α is the gain of the detector, and g and σ are the mean and the standard deviation of the read-out noise.

Deconvolution

- … or deblurring
- Take observed signal,
- and approximate blurring function,
- and invert the blurring
- in order to obtain the original or ideal signal
- Usual principle:
- Redistribute image flux, iteratively, taking blurring function into account

59

Hubble Space Telescope
Image restoration for tackling the spherical aberration problem between 1990 and 1993

- Concept of space telescope advanced by Lyman Spitzer Jr. (Princeton) in 1940s.
- First official mention by NASA in 1962, four years after NASA founded. Science team established by NASA in 1973. From 1975 ESA involved. Congress approved in 1978. Marshall (Huntsville) – construction, Goddard (Greenbelt) – science and ground control.
- Lockheed – basic spacecraft, Perkin-Elmer – primary mirror, ESA (BAe) – solar panels.
- 1986/1/26 – Challenger disaster.
- HST deployed in low Earth orbit – 600 km – by Discovery (STS-31) on 1990/4/25.
- First refurbishment mission Endeavour STS-61 in December 1993.

60

Supernove SN87A
HST image,
spherically aberrated,
original, histogram equlaized

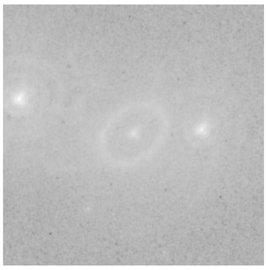

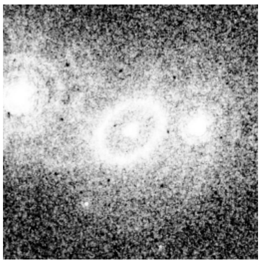

61

Point spread function
at original dynamic range
and histogram equalized

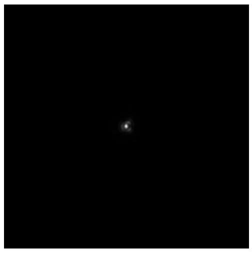

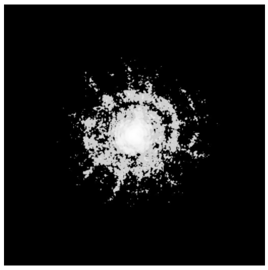

62

Deconvolution

Observed data: I(x,y)
Real image: O(x,y)
Assume: linear, shift-invariant imaging system

Then:
I(x,y) = (O * P)(x,y) + N(x,y)
where P is point spread function, N is noise,
and * is convolution

Solve for O using coupled relations:
$\mathbf{O^{n+1} \leftarrow O^{n}\ [\ (I/I^{n}) * P^{*}\ ]}$
$\mathbf{I^{n} \leftarrow P * O^{n}}$
where P* is conjugate of PSF

- Richardson, 1972, optical engineering literature
- Lucy, 1974, astronomy literature
- Shepp and Vardi, 1982, medical imaging literature
- Maximum likelihood solution, formally EM algorithm

63

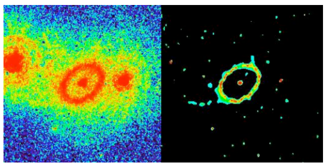

SN87a before (left) and after (right) deconvolution.
Both images histogram equalized and false colour coded.

64

Novelty – regularization through wavelet-based denoising

- The problem with the traditional way of doing this is that the algorithm thinks that each and every noise spike is deserving of getting flux back, which has been blurred in its vicinity.
- "Regularization" is the term used for an imposed constraint to stop the algorithm doing this.
- Wavelet-based noise filtering: take $\mathbf{R^n = I - I^n}$, i.e. $\mathbf{R^n = I - (P * O^n)}$**, the observed image, I, minus the image we would observe if we were to use the current estimate of the ideal image,** which defines the residual at each iteration. Take $\mathbf{R^n}$ into wavelet space (known for its energy compacting properties). Denoise in wavelet space and inverse transform into direct space. Continue iterations. This allows a noise-"cleaned" version of $\mathbf{I^n}$, while retaining and protecting signal.
- This is a computationally straightforward intervention at each iteration, based on the noise model used for the image. (E.g. widely-used CCD detectors have Gaussian read-out noise, together with Poisson photon noise.) Effective and efficient.

65

A Short Look at Ridgelet and Curvelet Transform Applications

66

Visual Display Balance and Contrast

- "Retinex" – retina + cortex – transform colour space to improve contrast.
- Multiscale retinex using wavelet transform.
- Applications:

(i) standard presentation of colour images on the web or in other display media;
(ii) canonical presentation of medical images;
(iii) standard for virtual environments in training.

67

J. Vermeer, "Lady writing a letter with her maid", 1670.

68

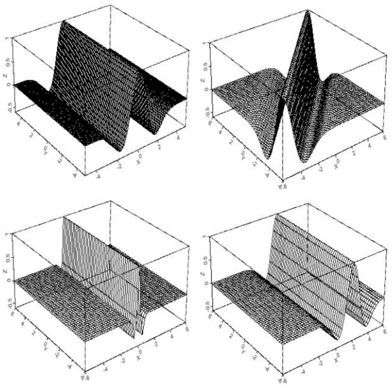

Figure 20.2: A few ridgelets.

69

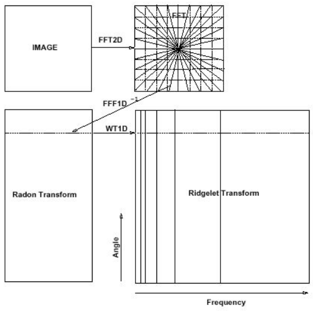

Figure 20.4: Ridgelet transform flowgraph. Each of the $2n$ radial lines in the Fourier domain is processed separately. The 1D inverse FFT is calculated along each radial line followed by a 1D nonorthogonal wavelet transform. In practice, the one-dimensional wavelet coefficients are directly calculated in the Fourier space.

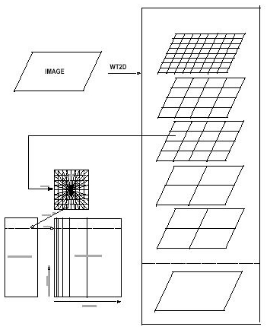

Figure 20.9: Curvelet transform flowgraph. The figure illustrates the decomposition of the original image into subbands followed by the spatial partitioning of each subband. The ridgelet transform is then applied to each block.

1. Apply the à trous algorithm with J scales,
2. set $B_1 = B_{min}$,
3. for $j = 1, \ldots, J$ do,
   (a) partition the subband w_j with a block size B_j and apply the digital ridgelet transform to each block,
   (b) if j modulo $2 = 1$ then $B_{j+1} = 2B_j$,
   (c) else $B_{j+1} = B_j$.

The sidelength of the localizing windows is doubled *at every other* dyadic subband, hence maintaining the fundamental property of the curvelet transform which says that elements of length about $2^{-j/2}$ serve for the analysis and synthesis of the j-th subband $[2^j, 2^{j+1}]$. Note also that the coarse description of the image c_J is not processed. Figure 20.9 gives an overview of the organization of the algorithm.

This implementation of the curvelet transform is also redundant. The redundancy factor is equal to $16J+1$ whenever J scales are employed. Finally, the method enjoys exact reconstruction and stability, because this invertibility holds for each element of the processing chain.

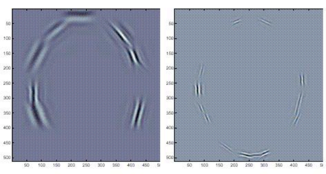

Figure 20.10: A few curvelets.

72

Figure 20.10 shows a few curvelets at different scales, orientations and locations.

Curvelet transform filtering

- RGB → LUV
- Apply curvelet transform to 3 bands
- Use sqrt of sum of squares (Euclidean norm)
- Filter
- Inverse curvelet transform
- LUV → RGB

73

Left: original. Right: filtered using curvelet transform

74

Left: original. Right: filtered using curvelet transform

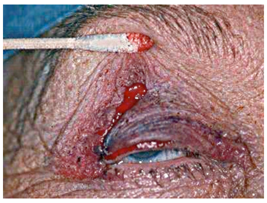

75

Compression

- Use a pyramidal transform (so: a wavelet transform with decimation)
- Or a non-wavelet, multiresolution, transform, e.g. pyramidal median transform
- Incorporate noise modeling for e.g. CCD detectors
- Quantize, entropy encode
- Essential principle here: noise is inherently non-compressible, so separate out noise from signal

76

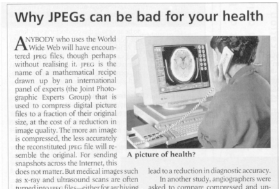

Why JPEGs can be bad for your health

ANYBODY who uses the World Wide Web will have encountered JPEG files, though perhaps without realising it. JPEG is the name of a mathematical recipe drawn up by an international panel of experts (the Joint Photographic Experts Group) that is used to compress digital picture files to a fraction of their original size, at the cost of a reduction in image quality. The more an image is compressed, the less accurately the reconstituted JPEG file will resemble the original. For sending snapshots across the Internet, this does not matter. But medical images such as x-ray and ultrasound scans are often

A picture of health?

lead to a reduction in diagnostic accuracy.

In another study, angiographers were

(The Economist, 2000/6/17)

Image compression is crucially important for image storage, transmission and display.
Astronomy and medical image are similar in that very often faint signal is of importance, and there are known noise models.

77

Digital Mammography

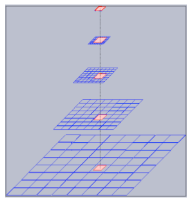

- A film, digitized at 42 microns, yields approx. a 4240 x 5670 16-bits-per-pixel image ≈ 50 MB.
- We use a wavelet pyramidal representation to support lossless compression, with very fast decompression by resolution level and by block.

78

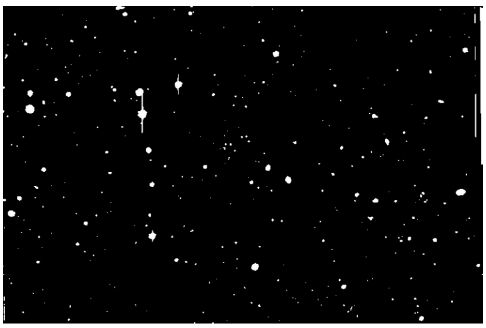

79

Indicative results of lossy and lossless large astronomy image compression

- 12,451 x 8268 MegaCam image (Canada-France-Hawaii Telescope, Hawaii). 412 MB greyscale image file.
- Visually-lossless compression took 10 minutes on workstation. Compressed to 4.1 MB i.e. < 1% of original size
- Decompression to resolution scale 5 (as shown) took 0.43 sec.
- Rigorously lossless compression took just over 3 minutes and resulted in a compressed file of size 97.8 MB, i.e. 23.75% of original size.

80